**DOI:** nprot.2016.101

**Editorial summary:** Cassaignau et al provide a strategy for large-scale production and analysis of translationally arrested, isotopically-labelled ribosome-bound nascent chains, enabling high-resolution co-translational protein folding studies using NMR spectroscopy.

**Proposed tweet: -** High-resolution #NMR analysis of co-translational #ProteinFolding [LINK]

**Proposed Ontology terms**
Biological sciences/Biochemistry/Protein folding
Biological sciences / Biological techniques / Structure determination / NMR spectroscopy / Solution-state NMR
Biological sciences/Molecular biology/Translation/Ribosome
Biological sciences/Biophysics/Biopolymers in vivo

**Keywords:**
solution-state NMR, NMR spectroscopy, ribosome, nascent chain, co-translational folding, ribosome-bound nascent chain complex, isotopic labelling, uniform labelling, selective labelling, protein folding, co-translational protein folding, structural analysis

**Supporting primary papers**

1. Cabrita, Lisa D., Cassaignau, Anaïs M.E., Launay, Hélène M.M., Waudby, Christopher A., Wlodarski, Tomasz, Camilloni, Carlo, Karyadi, Maria-Evangelia, Robertson, Amy L., Wang, Xiaolin, Wentink, Anne S., Goodsell, Luke S., Woolhead, Cheryl A., Vendruscolo, Michele, Dobson, Christopher M, Christodoulou, John. A structural ensemble of a ribosome-nascent chain complex during cotranslational protein folding. *Nat Struct Mol Biol* **23**, 278-285 (2016).

2. Deckert, A.W., Christopher A.; Wlodarski, Tomasz; Wentink, Anne S.; Wang, Xiaolin; Kirkpatrick, John P.; Paton, Jack F. S.; Camilloni, Carlo; Kukic, Predrag; Dobson, Christopher M.; Vendruscolo, Michele; Cabrita, Lisa D.; Christodoulou John Structural characterization of the interaction of α-synuclein nascent chains with the ribosomal surface and trigger factor. *Proceedings of the National Academy of Sciences* **113**, 5012-5017 (2016).

3. Waudby, C.A., Launay, H., Cabrita, L.D. & Christodoulou, J. Protein folding on the ribosome studied using NMR spectroscopy. *Progress in nuclear magnetic resonance spectroscopy* **74**, 57-75 (2013).

**Permissions required for:**
Figure 4
Supplementary Figure 1

---

# A strategy for co-translational folding studies of ribosome-bound nascent chain complexes using NMR spectroscopy

Anaïs M.E. Cassaignau[1]*, Hélène M.M. Launay[1]*, Maria-Evangelia Karyadi[1], Xiaolin Wang[1], Christopher A. Waudby[1], Annika Deckert[1], Amy L. Robertson[1], John Christodoulou[1†] and Lisa D. Cabrita[1†]

[1]Institute of Structural and Molecular Biology, University College London and School of Crystallography, Birkbeck College, University of London, Gower Street, London WC1E 6BT

*These authors contributed equally to this work

† To whom correspondence should be addressed:
John Christodoulou (JC) j.christodoulou@ucl.ac.uk and Lisa D. Cabrita (LDC) tel: +44 (0)20 7679 2375

**Abstract**
During biosynthesis on the ribosome, an elongating nascent polypeptide chain can begin to fold, in a process central to all living systems. Detailed structural studies of co-translational protein folding are now beginning to emerge; such studies were previously limited, at least in part, by the inherently dynamic nature of emerging nascent chains, which precluded most structural techniques. Nuclear Magnetic Resonance (NMR) spectroscopy is able to provide atomic-resolution information for ribosome-nascent chain complexes (RNCs), but requires significant quantities (≥10 mg) of homogeneous, isotopically-labelled RNCs. Further challenges include limited sample working concentration and stability of the RNC sample (which contribute to weak NMR signals) and resonance broadening caused by attachment to the large (2.4 MDa) ribosomal complex. Here, we present a strategy to generate isotopically-labelled RNCs in *E. coli* that are suitable for NMR studies. Uniform translational-arrest of the nascent chains is achieved using an arrest motif, and isotopically-labelled RNCs are produced at high yield using high cell density *E. coli* growth conditions. Homogeneous RNCs are isolated by combining metal affinity chromatography to isolate ribosome-bound species with sucrose density centrifugation to recover intact 70S monosomes. Sensitivity-optimised NMR spectroscopy is then applied to the RNCs, combined with a suite of parallel NMR and biochemical analyses to cross-validate their integrity, including RNC-optimised NMR diffusion measurements to report on ribosome-attachment *in situ*. Comparative NMR studies of RNCs with the analogous isolated proteins permit a high-resolution description of the structure and dynamics of a nascent chain during its progressive biosynthesis on the ribosome.

**Introduction**

An emerging nascent polypeptide chain is extruded from the ribosome from its N- to C-terminus and is able to adopt its biologically active structure in a co-translational fashion[1, 2]. This process has been explored kinetically through biochemical studies, including pulse-chase investigations that are typically coupled to observations of proteolytic cleavage[3] or disulphide bond detection[4], which show that protein folding on the ribosome can be coupled to translation on the biological timescale. A high resolution understanding of how emerging nascent chains may adopt conformations on the ribosome, however, has been largely underpinned by biochemical and biophysical experiments carried out on translational-arrested ribosome-nascent chain complexes (RNCs). Key to these latter studies is the ability to achieve selective and uniform translational arrest using peptidic motifs; these motifs directly interact with the ribosome[5] during biosynthesis to stably retain a nascent chain of uniform length relative to the 3' truncated non-stop mRNA[6, 7]. In the case of 70S ribosomes from *E. coli*, peptidic motifs derived from the *E. coli* proteins TnaC[8] and SecM[1, 9-12] have been successfully exploited to produce homogeneous RNCs by generating thermodynamic snapshots of the emerging nascent chain at different stages of its biosynthesis[10]. While the conformational preferences of an emerging nascent chain will be

under kinetic control, where rates of translation compete with rates of folding the use of stalled RNCs has enabled important advances in our understanding of their acquisition of biologically active structure[13,14]. This has typically been reported using biochemical approaches including antibody recognition studies[15, 16] and limited proteolysis[17] in studies of several multi-domain proteins[18-21]. FRET studies of RNCs have been particularly fruitful in exploring nascent chain emergence and folding, highlighted in the study of an N-terminal domain of HemK, which was shown to sample a compact state prior to adopting its fold[22], and the demonstration of sequential formation of subdomains within NBD1 of the multi-domain protein CFTR[7]. FRET[23] has also been central to examination of early chain compaction within the exit tunnel, as has the development of cysteine-mass tagging PEGylation experiments[18]; together data generated by these techniques have suggested that nascent chains are able to form rudimentary structures such as $\alpha$-helices and $\beta$ turns[23, 24] as they traverse the ribosomal exit tunnel.

That differences exist between co-translational folding and the reversible folding of isolated proteins was initially well-illustrated in the cases of firefly luciferase[18] and tailspike protein[19]: as isolated proteins, they are unable to fold reversibly from a chemically denatured state, yet as RNCs, they showed the capacity to adopt native structure co-translationally during progressive emergence on the ribosome. It has been suggested that the efficiency of folding on the ribosome may in part be influenced by the effects of the ribosomal surface[25, 26], for which marked differences in folding rates have been observed in optical tweezer experiments of T4 lysozyme RNCs[25]. In addition, the distribution of synonymous and non-synonymous codons[21, 27] in the mRNA sequence alters the rate of nascent chain biosynthesis and, concomitantly, the rate and efficiency of folding[7, 28, 29]. In addition, the emerging nascent chain encounters a range of ribosome-associated auxiliary factors in the crowded cellular environment, the most pertinent for co-translational folding being the molecular chaperone trigger factor[4, 30, 31], whose proposed interactions are both nascent chain length- and sequence-dependent and likely shape the folding landscape available to the nascent chain.

Despite the possible influences that co-translational folding events may have in promoting efficient folding, a structural understanding of how this process is achieved on the ribosome is lacking. Underpinned by comprehensive studies of the functional ribosome using X-ray crystallography and cryo-EM[9, 32-37], high-resolution structural studies of RNCs using cryo-EM[8, 9, 38] and NMR spectroscopy[10, 39-41] are beginning to provide more detailed structural descriptions of the conformations sampled by ribosome-bound nascent chains. Cryo-EM reconstructions of RNCs have in some cases, for example, revealed nascent chain compaction and $\alpha$-helix formation within the ribosomal exit tunnel[38] and, more recently, the formation of a simple tertiary motif[42]. The steric restrictions imposed by the ribosomal exit tunnel[34], however, result in tertiary structure only forming beyond the tunnel in the majority of cases, where the dynamic nature of the ribosome-bound nascent chain impedes its observation via cryo-EM. A

structural understanding of the nascent chain remains experimentally challenging due to its inherently dynamic character and studies of such conformations are only possible through the use of NMR spectroscopy[10, 39, 40], a technique uniquely poised to offer both structural and dynamical information. Indeed, despite the large molecular weight (2.4 MDa) of the 70S ribosome complex, which contributes to significant broadening of the majority of its NMR signals[43, 44], ribosome-bound nascent chains display comparatively sharp and intense resonances such that detailed systematic structural studies of nascent chain folding on the ribosome are now emerging[1, 10, 39, 40]. These have been made possible by advances in preparative biochemistry methods for the production of large quantities of homogeneous RNCs. *In vitro* transcription-translation strategies[9, 39], but also the more recently developed *in vivo* approaches using selective and uniform translational arrest, have enabled the production of isotopically-labelled RNCs specifically for NMR studies[10, 45].

Much of our current understanding of co-translational folding has been derived from biochemical and biophysical studies of RNCs, which offer the advantage over NMR studies in that they can report on kinetic rates as monitored in real-time, however structural changes are typically inferred from single-site fluorescence probes on the nascent chain or through nascent chain interactions with reporter molecules. NMR spectroscopy of RNCs has, therefore, a significant advantage in its capacity to directly report upon structure, but describing co-translational protein folding at a residue-specific level. Its capacity to report on the highly dynamic nascent chain beyond the ribosomal tunnel means that it is uniquely positioned to complement structural techniques such as cryo EM to generate a high-resolution understanding of structure formation as it occurs during biosynthesis.

Here, we present an approach that can be used to describe conformations adopted by nascent chains during translation, based on methods used in our laboratory in studies of over 50 nascent chain samples of varying length and different sequences; our studies of an Ig-fold,[1, 10, 39, 40,46] and of an intrinsically disordered polypeptide (alpha-synuclein[47]) have been of particular value in developing our methodology. The protocol describes the *in vivo* production of isotopically-labelled RNCs, a biochemical approach for sample characterisation and a guide for NMR data acquisition and subsequent analysis in order to describe conformations adopted by nascent chains during translation. Rigorous approaches to monitor sample integrity are also outlined. This protocol will serve as an essential foundation for detailed studies of co-translational folding, allowing an understanding of the conformational dynamics of a ribosome-bound nascent chain, and serving to provide molecular restraints for molecular models at atomic resolution[1].

**Development of the Procedure**

We have designed an approach to produce homogeneous and isotopically-labelled RNCs *in vivo* through the manipulation of *E. coli* growth to generate large quantities of translationally-active ribosomes; this was achieved by using high-cell density growth conditions adapted from auto-induction procedures[48]. The isolation of large amounts of translating ribosomes relies on well-established separation techniques-- the sedimentation of ribosomal complexes using sucrose density ultracentrifugation[49]. We further adapted this technique for selection and purification of ribosome-bound nascent chains[10] at the high yields required for NMR spectroscopy relative to other structural and biophysical techniques;. ~10 mg of material is required per NMR sample which is roughly 2 to 3 orders of magnitude greater than that required for cryo-EM. We generate RNCs of different nascent chain lengths by varying the distance separating the protein of interest from the ribosome's peptidyl transferase centre (PTC), thereby producing successive snapshots along the co-translational folding pathway and enabling us to monitor both unfolded and folded conformations using equilibrium measurements. By evaluating variables including the sequence determinants and polypeptide chain length-dependent acquisition of structure during biosynthesis, we are developing structural models of co-translational protein folding.

NMR studies of RNCs are challenging for reasons that include the high viscosity of ribosomal solutions (with ideal working concentrations for NMR of ~10 μM, 24 mg/mL), but a significant limitation results from the inherent instability of the ribosomal complex, which is prone to degradation over extended periods of time. Ribosome-bound nascent chains can also be released from the ribosomal particle through mechanisms that include the overcoming of SecM stalling via spontaneous translocation[50, 51] or by the action of trace amounts of proteases. We have therefore adapted translational diffusion measurements from our NMR studies of ribosomes[43] to carefully monitor nascent chain integrity during NMR acquisition, and complemented these with an orthogonal approach using biochemical assays to validate our observations.

The NMR strategy presented here should guide the reader towards the production of RNCs and detailed structural studies of co-translational folding events as they occur during biosynthesis on the ribosome, as we have undertaken for FLN5[1, 10, 40, 52] and alpha-synuclein[47]. Combining RNCs with comparative studies of the analogous isolated proteins provides the means to understand the manner in which the ribosome modulates folding within living systems in conjunction with the array of cellular factors that are distinct from studies of protein folding in bulk solution.

**Overview of the Procedure**

Here, we describe the main steps involved in sample production and data analysis to report on structural conformations populated by nascent chains bound to the ribosome (Fig. 1).

DNA constructs are designed to generate RNCs of the protein of interest using an expression vector with a translational arrest motif, e.g. a pLDC-17 vector[10] (Fig. 1a) and an N-terminal purification tag e.g. a His tag. For the production of isotopically-labelled RNCs (Fig. 1a), high-cell density cultures of *E. coli* are grown (typically 0.5-2 L) to which isotopes are added at the induction of protein expression[10], in order to confine labelling to the nascent chain. For purification of the RNCs (Fig. 1a), the *E. coli* cells are lysed and the RNCs are recovered using a combination of purification methods involving, for example, metal affinity chromatography to an N-terminal tag (for His-tagged RNCs) and sucrose density centrifugation (Fig. 2a). Biochemical analyses of the purified RNCs using SDS-PAGE and western blot analyses (Fig. 1b and Fig. 2b-d) evaluate the homogeneity and integrity of the samples.

NMR experiments on RNCs (Fig. 1c) are typically performed using sample concentrations close to 10 μM, as the 70S complexes are less stable at higher concentrations and the associated increases in sample viscosity impacts on the observable NMR signal. A temperature is chosen that is suitable for the system in question, for example, reduced temperatures (e.g. 277 K, 283 K) favour sample stability, and are desirable for the study of disordered conformations as decreased amide/water proton exchange effects result in increased signal intensity[53]. Reducing the temperature also minimizes the background signal contribution from the globular ribosomal protein, bL12. By contrast, higher temperatures (e.g. 298 K) have the effect of decreasing the correlation times of folded proteins and therefore improving their NMR observability, but increasing temperatures to 310 K results in severe ribosomal degradation over short periods (minutes-hours). The exact parameters chosen for data acquisition therefore require consideration, as further outlined in Box 1, to maximise the observable signal and the quality of data. Typically for RNCs, heteronuclear experiments are recorded in an interleaved manner with translational diffusion NMR experiments that report specifically on sample integrity (Fig. 1c). Indeed, RNC lifetimes can vary considerably depending on their structural properties and the temperature at which they are recorded (e.g. on the order of days at 277 K, but only up to ~30 h at 298 K). Nascent chain degradation can significantly complicate the interpretation of RNC spectra as the presence of a comparatively small population of released nascent chain can give rise to sharp and intense resonances due to its much shorter correlation time[39].

The quality control analysis (Fig. 1c) of the ribosomal complex during NMR acquisition involves monitoring resonances corresponding to 70S ribosomal proteins in 1D experiments, and those corresponding to the nascent chain in 2D experiments. NMR signals can be monitored over time, where typically an increase in intensity is interpreted as nascent chain release from the ribosome, (which can be rationalised by the shortened correlation time that would be anticipated for a smaller species). Additionally, measurements of the translational diffusion coefficient, $D$, by NMR also exploit the large difference in $D$ between intact RNCs and degraded ribosome particles or released nascent chains (e.g. at 298 K, $D$ = 2.0 ± 0.3x10$^{-11}$ m$^2$s$^{-1}$ for a

ribosome-bound nascent chain and in our system $D$=1.3x10$^{-10}$ m$^2$s$^{-1}$ for isolated or released FLN5). Thus, to evaluate the integrity of the 70S ribosome, a combination of $^1$H 1D acquisition and $^1$H STE translational diffusion experiments (Fig. 3b, c) is used; the resonances observed in the methyl region of the $^1$H spectrum (0.7-1 p.p.m. in the $^1$H dimension, Fig. 3b) originate predominantly from the labile ribosomal bL12 protein[54-56] and can be used as an approximate measure of overall ribosomal integrity. Measurement of nascent chain attachment to the ribosome is, however, essential, and $^{15}$N XSTE or $^{13}$C-edited diffusion experiments are used to directly probe the nascent chain. In cases, however where the nascent chain may give rise to NMR signals too weak for diffusion measurements to be recorded within a suitable timeframe, changes in the average 2D intensities of the nascent chain can be used to monitor sample stability.

In parallel with NMR experiments, samples of the RNC collected throughout NMR acquisition are also probed using a western blot to evaluate the nascent chain integrity over time, using nascent chain-specific antibodies against the N-terminus (e.g. anti-His tag antibody) or the C-terminus (e.g. SecM stalling sequence). Ribosome-bound nascent chains typically migrate on SDS-PAGE with an additional 17-20 kDa band-shift relative to that of the expected molecular mass of the nascent chain; this is caused by the presence of a P-site peptidyl tRNA which is covalently linked to a stalled nascent chain (Fig. 2c). To distinguish intact RNCs from those that have been compromised by nascent chain release, we carry out polyacrylamide gel electrophoresis using low pH conditions that preserve the nascent chain-tRNA ester bond. With these tools in hand, we are able to confidently report spectra of intact RNCs for structural analysis, including detailed analyses of resonance intensities and linewidths, to explore the relaxation properties and mobility of the nascent chain. Together, these studies are used to describe differences between folding in bulk solution and on the ribosome.

**Advantages and Limitations**

Our protocol presents a versatile *in vivo* approach using *E. coli* for the production of significant quantities of homogeneous RNCs, which can be adapted to incorporate isotopic labelling schemes as necessary for studies using NMR spectroscopy. The capacity to exploit *E. coli* in this manner enables the production of uniformly-arrested RNCs comparable to those produced using *in vitro* translation methods, using routine biochemical reagents, and at a relatively low cost. While the use of stable isotopes for nascent chain labelling introduces a significant cost, it is arguably, a reasonable compromise for the rich, residue-specific information that can be derived from a single RNC spectrum.

An important consideration, however, in using an *in vivo*-based approach for isotopic labelling of RNCs is the extent to which the labelling is confined to the nascent chain. Continuous ribosome biogenesis can result in background 70S ribosome labelling, which gives rise to

resonances that correspond to the bL12 ribosomal stalk observable in 2D correlation spectra[43] alongside labelled nascent chains. Typically however, the high cell density conditions during the induction of expression restricts cell growth (and thus ribosome biogenesis), and the use of rifampicin, an inhibitor of the bacterial host DNA polymerase, reduces the extent of bL12 isotopic labelling (by an additional ~10% in our hands). Our protocol also describes NMR measurements (step 24) in order to quantify ribosome background labelling in samples that are uniformly $^{15}$N and/or $^{13}$C-labelled.

The procedure has been designed to enable RNCs to be produced in a straightforward manner, however the most significant challenges arise from the inherent complexities presented by the samples themselves during NMR studies. Notably, these include the low maximum achievable RNC concentrations and their high molecular weight, the necessity for continuous assessment of the sample's integrity and the physical properties of the nascent chains themselves. This prompts the need for a careful choice of nascent chain system (see *Experimental Design*) as well as NMR experimental design (*Box 1*), and complementary comparative studies with the isolated protein. We anticipate that the continuous development of NMR strategies to enhance sensitivity, as well as the molecular biology of RNCs will improve further the capacity to study co-translational folding in this manner.

## Experimental Design

**Choosing a nascent chain system to study.** For NMR studies of RNCs, a key factor is the choice of the nascent polypeptide to investigate, which is strongly influenced by the dynamic properties of the nascent chain and its interactions with the ribosome. Relative to the isolated polypeptide in bulk solution, the ribosome-attached nascent chain has decreased motional properties, which result in a reduction in its NMR signal, and which can be diminished further by interactions between the nascent chain and the ribosomal surface, or by possible intra-chain interactions. As NMR has the capacity to report on transient and/or weak interactions, any significant affinity between the nascent chain of interest and the ribosomal surface manifests as resonance broadening and/or changes in chemical shift. Our protocol has, to date, been applied to polypeptides that inherently give rise to strong NMR signals (i.e. proteins of small size (<30 kDa) and/or of disordered nature) and to those that that show a high spectral quality in both their natively folded and unfolded forms even in the presence of 70S ribosomes (Supplementary Fig. 1). A characterisation of the polypeptide of interest in isolation, in both its folded and unfolded forms (achieved e.g. by mutation or C-terminal truncation), and in the presence of 70S ribosomes, is instructive of a suitable nascent chain choice for NMR investigation; it also forms an important basis for comparative analysis relative to RNCs. In addition, it is advantageous to choose a nascent chain system where the polypeptide has biochemical properties that can be evaluated. A range of biochemical and biophysical strategies have been used to characterise

ribosome-nascent chain complexes (e.g. enzymatic activity[14], antibody recognition[15, 16], limited proteolysis[17], PEGylation[1, 57]), as well as to consider the unique influence of the cellular milieu during biosynthesis[31, 58, 59]. The use of combined approaches permits potential corroboration of the high-resolution NMR studies of RNCs with co-translational events as they take place within the cell.

**Choice of isotopic labelling scheme.** The choice of a suitable isotopic labelling scheme constitutes an important part of the experimental design to ensure optimal observability of the nascent chain, as shown in our studies of FLN5 RNCs[1, 10, 39, 40, 60]. For the study of disordered conformations, $^{15}N$ labelling can take advantage of the large dispersion in the $^{15}N$ dimension, as its chemical shift is particularly sensitive to the local amino acid sequence rather than tertiary structure. $^{15}N$ spectra therefore typically resolve a larger number of resonances arising from disordered states as compared to other heteronuclei. In the study of globular states, $^{13}C$ labelling can typically provide the more sensitive probes needed to characterise the conformations present, in particular the formation of stable tertiary structure. Observation of NMR spectra for globular nascent chains however, present additional challenges through reduced flexibility and proximity to the ribosomal particle[10]. To overcome unfavourable relaxation properties that result in weak NMR signals in heteronuclear correlation spectra, selective methyl side-chain labelling of the nascent chain combined with perdeuteration (achievable for the side chains of Ile, Leu, Val, Ala, Met, Thr [61, 62]; e.g. [U-$^{2}H$]; Ileδ1-[$^{13}CH_3$]) offers vast enhancements in NMR sensitivity[63], especially when paired with the methyl-TROSY effect inherent to the HMQC pulse sequence. With the increasing expense associated with perdeuteration and selective $^{13}CH_3$ isotopic labelling, the production of $^{1}H$-$^{15}N$ labelled RNCs would be a recommended first step to initially evaluate an RNC system prior to introducing the more involved selective labelling approaches.

## MATERIALS

### Reagents

CRITICAL: All reagents should be sourced at the highest possible grade. Unless otherwise indicated, most routine biochemical reagents can be sourced from the user's preferred supplier.

- *E. coli* expression vector for the RNC of interest (user generated)
- $^{15}NH_4Cl$ (98 atom % $^{15}N$) (sourced from e.g. Isotec, Cambridge Isotope Laboratories)
- Appropriate precursors for selective methyl labelling (e.g. 2-Ketobutyric acid-4-$^{13}C$ sodium salt hydrate for Ile labelling) (sourced from e.g. Isotec, Cambridge Isotope Laboratories)
- Antibiotics (e.g. ampicillin)
- BL21 (DE3) *E. coli* (e.g. Novagen, cat. no. 230132)
- BME vitamins 100x (Sigma-Aldrich cat. no. B6891)
- $CaCl_2$
- Deuterated glucose (D-Glucose-1,2,3,4,5,6,6-$d_7$) (e.g. Sigma Isotec, cat. no. 552003)
- Deuterium oxide ($D_2O$) (99.8 atom % D) (e.g. Sigma Isotec, cat. no. 617385)
- D-Glucose

· Isopropyl β-D-1-thiogalactopyranoside (IPTG)
· $KH_2PO_4$
· L-aspartic acid
· $MgSO_4$
· NaCl
· $Na_2HPO_4$
· $Na_2SO_4$
· Rifampicin
· Trace metals: $CoCl_2$, $CuCl_2$, $NiCl_2$, $Na_2SeO_3$, $Na_2MoO_4$, $H_3BO_3$, $ZnSO_4$, $MnCl_2$, $FeCl_2$
· Yeast nitrogen base (e.g. Difco, cat. no. 233520)
· Adenosine Triphosphate (ATP)
· 2-Mercaptoethanol (BME)
· 4-(2-Hydroxyethyl)-1-piperazineethanesulfonic acid-$d_{18}$ (HEPES-$d_{18}$) (98 atom % D) (sourced from e.g. Isotec, Cambridge Isotope Laboratories)
· 4,4-dimethyl-4-silapentane-1-sulfonic acid (DSS)
· Bradford's Reagent
· EDTA-free protease inhibitor cocktail tablets (e.g. cOmplete, Mini, EDTA-free Protease Inhibitor Cocktail Tablets, Roche cat. no. 04 693 159 001)
· Ethylenediaminetetraacetic acid (EDTA)
· HEPES
· Imidazole
· Lysozyme
· Magnesium acetate
· $MgCl_2$
· Potassium acetate
· DNase I (RNase free)
· Ultra pure sucrose (e.g. UltraPure Sucrose, Invitrogen cat. no. 15503-022)
· Metal affinity resin (e.g $Ni^{2+}$)
· 10, 12 or 15% (w/v) Bis-Tris polyacrylamide gel (e.g. Invitrogen or hand-cast)
· MOPS running buffer (e.g. Invitrogen cat. no NP0001)
· Silver staining kit
· Bis-Tris
· Bromophenol Blue
· Dithiothreitol (DTT)
· Glycerol
· Sodium Dodecyl Sulphate (SDS)
· Molecular weight marker
· RNC specific antibodies (e.g. anti-His, anti-SecM)
· Blocking reagents (e.g. skim milk powder)
· Nitrocellulose membrane
· Enhanced chemilluminescence (ECL) reagents
· Glycine
· Methanol
· RNase A
· Sodium dodecyl sulphate (SDS)
· Tris-Base
· Tween-20
· Western blot molecular weight marker

**Equipment**

- Centrifuge(s) capable of speeds of 4,000 x g, and 18,000 x g
- Density gradient fractionation system for pouring and fractionation of sucrose gradients (e.g. Teledyne Isco Foxy Jr Fraction Collector coupled a pump e.g. Watson Marlow 313S pump)

- French Press or equivalent high pressure cellular disruption equipment
- Software for NMR data processing, e.g. NMRPipe[64] and further analysis, such as Sparky 3.115 (T. D. Goddard and D. G. Kneller, SPARKY 3, University of California, San Francisco) or CcpNmr Analysis v.2.241[65].
- Software for statistical analysis and data visualization, eg MATLAB R2014a (MATLAB and Statistics Toolbox Release 2012b, The MathWorks, Inc., Natick, Massachusetts, United States) or Mathematica Wolfram (Wolfram Research, Inc., Mathematica, Version 10.4, Champaign, IL (2016))
- Ultracentrifuge(s) equipped with suitable rotors (e.g Type45 Ti, SW28 (Beckman))
- NMR spectrometer. As sensitivity is a major limiting factor, a cryogenic probehead is essential and a magnetic field strength corresponding to a $^{1}H$ frequency ≥700 MHz is recommended (e.g. Bruker Avance III)
- NMR tubes 5 mm $D_2O$-matched Shigemi tubes (e.g. Bruker, BMS-005B)

REAGENT SETUP

**100% trace metals**: (2 mM $CoCl_2$, 2 mM $CuCl_2$, 2 mM $NiCl_2$, 2 mM $Na_2SeO_3$, 2 mM $Na_2MoO_4$, 2 mM $H_3BO_3$, 1 mM $ZnSO_4$, 1 mM $MnCl_2$, 20 mM $CaCl_2$, 50 mM $FeCl_3$) Prepare a 50 mL solution by adding 100 µL 1 M $CoCl_2$, 100 µL 1 M $CuCl_2$, 100 µL 1 M $NiCl_2$, 100 µL 1 M $Na_2SeO_3$, 100 µL 1M $Na_2MoO_4$, 100 µL 1 M $H_3BO_3$, 50 µL 1 M $ZnSO_4$, 50 µL 1 M $MnCl_2$, 1 mL 1 M $CaCl_2$, 2.5 mL 1 M $FeCl_3$ to $H_2O$ (or $D_2O$). Store at room temperature (stable for months).

**MDG medium:** For the production of ribosomes, adapted from[48]. Prepare MDG for uniform labelling (step 3A(i)) in $H_2O$. For perdeuteration (Procedure step 3B), prepare all components in deuterium oxide. For selective methyl labelling (steps 3B(i)-(iii)), use deuterated glucose, D-Glucose-1,2,3,4,5,6,6-$d_7$ instead of D-Glucose as specified. Filter sterilise all stock solutions prior to use and store at room temperature (stable for months).

| Component | Amount per L | Final concentration |
|---|---|---|
| 20% (w/v) D-Glucose (or D-Glucose-1,2,3,4,5,6,6-$d_7$) | 10 mL | 2 g/L |
| 1 M $MgSO_4$ | 2 mL | 2 mM |
| Trace metals (100%) | 200 µL | 0.02% |
| 1 M $Na_2HPO_4$ | 25 mL | 25 mM |
| 1 M $KH_2PO_4$ | 25 mL | 25 mM |
| 20% (w/v) $NH_4Cl$ | 5 mL | 1 g/L |
| 1 M $Na_2SO_4$ | 5 mL | 5 mM |
| $D_2O$ (or $dH_2O$) | 928 mL | |

**EM9 medium.** For expression of RNCs, adapted from[66]. For selective isotopic labelling of the nascent chain (step 3A(iii)), use $^{15}N$ $NH_4Cl$ ($^{15}N$ labelling) or $^{13}C$ glucose ($^{13}C$ labelling) as desired. For selective methyl labelling (step 3B(iv)), use D-Glucose-1,2,3,4,5,6,6-$d_7$ instead of D-Glucose. For perdeuteration (Procedure step 3B), prepare all components in deuterium oxide. Filter sterilise all stock solutions prior to use and store at room temperature (stable for months).

| Compound | Amount | Final concentration |
|---|---|---|
| 20% (w/v) D-Glucose (or $^{13}C$-Glucose or Glucose-1,2,3,4,5,6,6-$d_7$) | 10 mL | 2 g / L |
| 1 M $MgSO_4$ | 2.5 mL | 2.5 mM |
| Trace metals (100%) | 125 µL | 0.0125% (w/v) |
| 70 g/L $Na_2HPO_4$ | 100 mL | 7 g/L |
| 34 g/L $KH_2PO_4$ | 100 mL | 3.4 g/L |
| 5.8 g/L NaCl | 100 mL | 0.58 g/L |
| 20% (w/v) $NH_4Cl$ (or $^{15}N$ $NH_4Cl$) | 5 mL | 1 g/L |
| 1 M $CaCl_2$ | 200 µL | 0.2 mM |
| Yeast nitrogen base | 0.8 g | 0.8 g/L |
| $H_2O$ (or $D_2O$) | 682 mL | |

**EM9 salts.** Prepare a 100 mL solution by adding 10 mL 70 g/L $Na_2HPO_4$, 10 mL 34 g/L $KH_2PO_4$ and 10 mL 5.8 g/L NaCl into $H_2O$.

**Lysis buffer.** 1 M KOAc, 50 mM HEPES, 12 mM MgOAc, 5 mM EDTA, 5 mM ATP, 2 mM BME, 1 mg/mL lysozyme, and DNase I, protease inhibitors (as per manufacturer's instructions), pH 7.5. Prepare a 100 mL solution by adding 20 mL 5 M KOAc, 10 mL 0.5 M Hepes, 4.8 mL 0.25 M MgOAc, 1 mL 0.5 M EDTA, 250 µg ATP, 78 µL BME, 100 mg lysozyme, and traces of DNase I into $H_2O$. pH the solution using NaOH. Filter sterilise and chill prior to use.

**Resuspension Buffer.**1 M KOAc, 50 mM HEPES, 12 mM MgOAc, 5 mM EDTA, 5 mM ATP, 2 mM BME, pH 7.5. Prepare a 100 mL solution by adding 20 mL 5 M KOAc, 10 mL 0.5 M Hepes, 4.8 mL 0.25 M MgOAc, 1 mL 0.5 M EDTA, 250 µg ATP and 78 µL BME into $H_2O$. pH the solution using NaOH. Filter sterilise and chill prior to use.

**Washing buffer.** 500 mM KOAc, 50 mM HEPES, 6 mM MgOAc, 2 mM BME, pH 7.5. Prepare a 500 mL solution by adding 50 mL 5 M KOAc, 50 mL 0.5 M Hepes, 12 mL 0.25 M MgOAc and 390 µL BME into $H_2O$. pH the solution using NaOH. Filter sterilise and chill prior to use.

**Elution buffer.** 500 mM KOAc, 50 mM HEPES, 6 mM MgOAc, 150 mM imidazole, 2 mM BME, pH 7.5. Prepare a 250 mL solution by adding 25 mL 5 M KOAc, 25 mL 0.5 M Hepes, 6 mL 0.25 M MgOAc, 15 mL 2.5 M imidazole and 195 µL BME into $H_2O$. pH the solution using HCl. Filter sterilise and chill prior to use.

**Sucrose buffers.** Two stock solutions of 35% and 10% (w/v) sucrose in 1 M KOAc, 50 mM HEPES, 12 mM MgOAc, 5 mM EDTA, 2 mM BME, 0.1/100 mL protease inhibitor tablet, pH 7.5. Prepare for each a 500 mL solution by adding 175 g (or 50 g) of sucrose, 100 mL 5 M KOAc, 50 mL 0.5 M Hepes, 24 mL 0.25 M MgOAc, 5 mL 0.5 M EDTA, 390 µL BME and 0.5 protease inhibitor tablet into $H_2O$. pH the solution using NaOH. Filter sterilise and chill prior to use.

**Tico buffer.** 30 mM $NH_4Cl$, 10 mM HEPES (or deuterated HEPES-$D_{12}$), 12 mM $MgCl_2$, 1 mM EDTA, 2 mM BME, 0.1/100 mL protease inhibitor tablet, pH 7.5. Prepare a 100 mL solution by adding 2 mL of 0.5 M Hepes, 6 mL 0.5 M $NH_4Cl$, 2.4 mL 0.5 M $MgCl_2$, 0.2 mL 0.5 M EDTA, 156 µL BME and 0.1 protease inhibitor tablet into $H_2O$. pH the solution using NaOH. Filter sterilise and chill prior to use.

**Low pH loading dye.** Prepare 20 mL as tabulated below. Aliquot into 1 mL aliquots and store at -20°C (stable for years).

| Compound | Amount | Concentration |
|---|---|---|
| Glycerol | | 30% (v/v) |
| Bis-Tris pH 5.7 | | 0.25 M |
| Bromophenol Blue | | 0.04% (w/v) |
| DTT | | 0.8% (w/v) |
| SDS | | 8% (w/v) |

## PROCEDURE

### Generation of isotopically-labelled RNCs TIMING 2 weeks – 1 month

1. Using standard molecular biology techniques, introduce the gene coding for the polypeptide of interest together with the SecM stalling motif (150-FSTPVWISQAQGIRAGP-166; SecM numbering[12]) into an *E. coli* expression vector with a suitable N-terminal purification tag as desired.
2. Transform the DNA construct into BL21(DE3) *E. coli*, and use a single colony to inoculate 3 mL of LB media with antibiotics. Incubate the cells at 37°C and 180 rpm for 12 h.

3. Depending on the labelling strategy selected for a given nascent chain system (refer to *Experimental Design*), isotopically-label RNCs *in vivo* using *E. coli* according to *Option (A)* to achieve uniform labelling (EM9 medium can be adapted for e.g. U-$^{1}$H-$^{15}$N,$^{13}$C or U-$^{1}$H-$^{13}$C labelling – see Reagent Setup) or *Option (B),* to achieve perdeuteration and selective labelling of methyl sidechains. These two strategies can be used for implementing alternative labelling schemes. However, given the relative costs associated with isotopic labelling, it is likely that uniform labelling approaches (Option (A)) would be considered initially, prior to more complex labelling schemes (e.g. Option (B)).

*OPTION (A) Uniform U-$^{15}$N-labelling TIMING 2 d*

**i.** Inoculate 1 L of MDG medium with cells from step 2 to a starting $OD_{600nm}$ of 0.05-0.1/mL. Allow the cells to grow and reach saturation at 37°C, 180 rpm (~16-20 h) by monitoring $OD_{600nm}$ measurements.

**ii.** Pellet the cells at 2,200 x g, 25 min, 4°C and gently resuspend the cells into 1 L of 1 x EM9 salts. Repeat once, i.e. pellet the cells at 2,200 x g, 25 min, 4°C and gently resuspend the cells into 1 L of 1 x EM9 salts again.

**iii.** Pellet the cells at 2,200 x g, 25 min, 4°C and gently resuspend the cells in 1 L EM9 medium containing isotopes as desired (e.g. $^{15}$N $NH_4Cl$ and/or $^{13}$C-glucose) (see Reagent Setup) and induce expression of the polypeptide by adding IPTG to the medium to a final concentration of 1 mM.

**iv.** Incubate the cells at 37°C, 180 rpm. After 10 min, add rifampicin to a final concentration of 150 µg/mL.

**v.** Continue expression for 35 min at 37°C, 180 rpm and then harvest the cells by centrifugation (2,500 x g, 20 min, 4°C ). Either proceed to step 4, or store the cell pellet at -20°C.

**PAUSE POINT** This sample can be stored at -20°C for months.

*OPTION (B) Selective labelling of $^{13}CH_3$ groups TIMING 5-6 d*

<CRITICAL> The growth kinetics of *E. coli* using deuterated media components are significantly slower (doubling time of 1-1.5 h or more), hence the production time of RNCs using this strategy requires longer than that for protonated (e.g. $^{1}$H-$^{15}$N) approaches. Here, the *E. coli* are first grown in deuterium oxide using protonated carbon sources, followed by deuterated carbon sources, prior to large scale growth and expression; this generally improves the reliability in *E. coli* growth.

**i.** Adapt the cells into perdeuterated media, first into deuterated media (containing D-glucose) and then subsequently into deuterated media with deuterated glucose, as tabulated below. For each adaptive step, inoculate 5 mL medium to a starting $OD_{600nm}$ of 0.2-0.3/mL. Allow the $OD_{600nm}$ of the cells to reach saturation at 37°C and 180 rpm, which

can range between 20-24 h. After the final adaptive stage, centrifuge the culture at 2,500 x g, 20 min, 4°C.

| Adaptive step | Medium | Glucose source |
|---|---|---|
| 1 | MDG | D-Glucose |
| 2 | Perdeuterated MDG | D-Glucose |
| 3 | Perdeuterated MDG | D- Glucose-1,2,3,4,5,6,6-$d_7$ |

**ii.** Use the cells pelleted from the final adaptive stage at step 3B(i) to prepare a 100 mL culture in perdeuterated MDG, grow to saturation and centrifuge as described in step 3B(i).

**iii.** Use the cells pelleted from the culture in Step 3B(ii) to inoculate 500 mL of MDG and grow the cells using the conditions described in Step 3B(i).

**iv.** Pellet the cells at 3000 x g for 15 min and gently resuspend them in 500 mL of EM9 medium together with the appropriate precursors (see *Reagent Setup*) required for selective methyl labelling,

**v.** Grow cells at 37°C and 180 rpm and monitor cell growth until the cells have reached mid-log phase growth (once $O.D._{600}$ starts to increase).

**vi.** Induce expression of the RNC by adding IPTG to a final concentration of 1 mM and grow for 90 min at 37°C. Harvest the cells by centrifugation (2,500 x g, 20 min, 4°C), and either proceed to step 4 or store the cell pellet at -20°C. *CRITICAL STEP Rifampicin is omitted in the production of [U-$^{2}$H]; $^{13}CH_3$-labelled RNCs as we have found that it can have an adverse effect on RNC expression.*

**PAUSE POINT** This sample can be stored at -20°C for months.

**<u>Purification of labelled RNCs by metal affinity chromatography and sucrose density gradient centrifugation TIMING 3 d</u>**

<CRITICAL > Use gloves for steps 4-15 and keep all reagents and samples chilled to maintain the RNC integrity.

4. Thaw the cells at room temperature (22°C) and resuspend in Lysis Buffer (20 mL/L of cells). <CRITICAL STEP> Do not leave cells at room temperature for any longer than required for thawing to take place. Alternatively, the cells can be thawed on ice.
5. Lyse the cells by pressure in a French Press, 4-6 passes at 1000 psi. Keep the cells ice-cold between passes.
6. Spin the cellular debris at 40,000 x g, 4°C, 45 min. If the supernatant is not clarified completely, transfer the supernatant to a new tube and repeat the centrifugation.
7. Load the clarified supernatant onto an ice-cold 35% (w/v) sucrose cushion. Spin the sucrose cushion at 200,000 x g, for 4-12 h, in an ultracentrifuge (Type 45Ti rotor,

Beckman). *Optional: Retain the resulting supernatant to purify the released nascent chain if desired e.g. to compare bound versus released nascent chains by NMR, (e.g. using metal affinity chromatography with the user's resin of choice, according to manufacturer's instructions).*

8. Gently resuspend the ribosomal pellet in Resuspension Buffer and measure the ribosome concentration by $OD_{260nm}$ (1 $OD_{260nm}$ = 24 pmol / mL). <CRITICAL STEP> If using a pipette to resuspend the pellet, avoid excess bubble formation to minimize potential release of the nascent chain.
9. Bind the ribosomal suspension to an appropriate metal affinity resin according to manufacturer's instructions for 1 h at 4°C.
10. Wash the resin with Washing Buffer, according to manufacturer's instructions, until the protein detected in the flowthrough is negligible as determined visually using a Bradford assay.
11. Elute the RNC fraction with Elution Buffer, assessing when elution is complete as described in Step 10 (typically 50-100 mL).
12. Concentrate the eluate in a 100 kDa cut-off concentrator according to manufacturer's instructions, to a 70S ribosome concentration of up to 10 nmol/mL (see Step 8), at 3,000 x g and 4°C. <CRITICAL STEP> For an accurate measure of the $OD_{260nm}$, the imidazole should be removed using the 100 kDa cut-off concentrator and progressively diluting the imidazole concentration.
13. Using a gradient former, pour 10-35% (w/v) sucrose gradients (35 ml, in 25x89 mm tubes) and load ≦1,500 pmol of the RNC from step 12. Spin the gradients in an ultracentrifuge at 64,000 x g, for 16-18 h.
14. Using a pump and fraction collector, fractionate the gradients (1.0-1.5 mL) and monitor elution using $OD_{254nm}$ measurements. Run aliquots (15 µL) from each fraction on a 12% (w/v) polyacrylamide gel and determine the presence and homogeneity of the 70S RNC peak (as shown in Figure 2b). ?TROUBLESHOOTING
15. Buffer exchange the 70S containing fractions using a 100 kDa cut-off concentrator to dilute the sucrose content to the nanomolar concentration range using Tico buffer at 3,000 x g and 4°C. Measure the absorbance of the RNCs at $OD_{260nm}$ and $OD_{280nm}$ to evaluate the 70S content (see Step 8) and its homogeneity using $OD_{260/280nm}$ ratio (expected range: 1.9-2.0)[67]. The resulting RNC sample can be used immediately or flash-frozen using liquid $N_2$ and stored at -80°C.

**PAUSE POINT** This sample can be stored at -80°C for months.

**<u>Biochemical analysis of the purified RNC samples TIMING 2 d</u>**

16. Prepare or purchase neutral pH gels with a polyacrylamide concentration that permits resolution of the nascent chain of interest and prepare the low pH loading dye. <CAUTION> Wear gloves when handling polyacrylamide, which is a neurotoxin.
17. To assess the RNC integrity and nascent chain occupancy, load the polyacrylamide gels with: 2-10 pmol samples of: untreated RNC (from step 15); RNC (from step 15) treated with 10 µg RNase A to digest the ribosomal RNA (at room temperature for 5 min), along with a series of concentration standards of the isolated protein of interest.
18. Using standard western blot procedures, transfer the gels onto a nitrocellulose membrane and probe with an antibody that recognises the RNC (e.g. anti-His, anti-SecM) and detect using chemilluminescence [68] <CRITICAL STEP> Minimise direct contact with nitrocellulose membrane to avoid cross-contamination.
19. Using ImageJ software, quantify the nascent chain occupancy by densitometry analysis: Measure the intensity of the chemilluminescent signal arising from the isolated protein standards and generate a standard curve. Determine the concentration of nascent chain present in the RNase A-treated RNCs using the standard curve of the isolated protein and the concentration of the RNCs (based upon the 70S concentration at $OD_{260nm}$). Note that a similar procedure can be applied for detecting the presence of trigger factor and any other ribosome/nascent chain associated proteins. ?TROUBLESHOOTING

**NMR data acquisition and parallel biochemical experiments TIMING 1-2 d**

20. After thawing the RNC sample (from step 15) on ice use a 100 kDa concentrator and Tico buffer to remove any released nascent chain using a buffer exchange. Measure the 70S ribosome concentration at $OD_{260nm}$. For selectively protonated samples, buffer exchange in Tico Buffer in $D_2O$ with deuterated HEPES.
21. Transfer approximately 10% of the RNC sample to a separate tube and incubate at the same temperature as used for NMR acquisition for the duration of NMR acquisition. Collect aliquots at regular intervals (e.g. hourly) for subsequent western blot analysis of RNC integrity over time (see Box 2).
22. Supplement the remainder of the RNC sample from step 21 with 10% (v/v) $D_2O$ and 0.001% (w/v) DSS and load 300 µL into a Shigemi tube and begin NMR acquisition as detailed in steps 23 and 24.
23. For uniformly $^{15}N$ and/or $^{13}C$-labelled samples only: Acquire experiments as tabulated below. Use the spectra produced in the $^{15}N$ edited and $^{15}N$ filtered experiments to identify the resonances arising from the ribosome in the amide region (7-9 p.p.m., $^{15}N$-labelled samples) or the methyl region (0.7-1 p.p.m. ,$^{13}C$-labelled samples). The percentage of background labelling from the relative amount of bL12 resonance intensities can be calculated as observed in either spectra.

| Type of experiment | Purpose | Analysis step(s) |
|---|---|---|
| $^{15}$N-edited $^{1}$H-$^{15}$N SOFAST HMQC | Record the first increment | The species observed in this experiment are $^{15}$N-bound protons. |
| $^{15}$N-filtered $^{1}$H-$^{15}$N SOFAST HMQC | Record the first increment | The species observed in this experiment are $^{14}$N-bound protons. |
| $^{15}$C-edited $^{1}$H-$^{13}$C SOFAST HMQC | Record the first increment | The species observed in this experiment are $^{13}$C-bound protons. |
| $^{13}$C-filtered $^{1}$H-$^{13}$C SOFAST HMQC | Record the first increment | The species observed in this experiment are $^{12}$C-bound protons. |

24. Acquire the NMR experiments detailed in the table below in an interleaved manner (refer to Box 1 for further details concerning the NMR experimental design): ?TROUBLESHOOTING

| Type of experiment | Purpose |
|---|---|
| $^{1}$H 1D experiment | Monitor the amide region (7-9 p.p.m.), ribosomal resonances in the methyl region (0.7-1 p.p.m.), buffer resonances. |
| 2D $^{15}$N-$^{1}$H or $^{13}$C-$^{1}$H correlation experiment | Obtain spectra reporting on nascent chain conformations and dynamics. |
| Heteronuclear diffusion: E.g. $^{15}$N XSTE diffusion[38], SORDID diffusion[60, 69] or $^{13}$C-edited STE diffusion[39] experiment | Monitor the diffusion coefficient associated with the resonances observed in 2D experiments and from this assess the nascent chain attachment to the ribosome. |
| $^{1}$H STE diffusion experiment | Monitor the diffusion coefficient associated with the methyl resonances in 1D experiments and from this assess the integrity of the ribosome. |

**Analysis of RNC sample integrity over time TIMING 2 d**

25. **Analysis of $^{1}$H 1D spectra to evaluate ribosomal resonances.** Process each $^{1}$H 1D spectrum and analyse resonances (methyl resonances, 0.7-1.0 p.p.m.) specifically arising from the ribosomal background (mainly from protein bL12) and buffer components such as

HEPES (2.6-3.8 p.p.m.). Note the timeframe during which the signals remain unchanged. We typically process the spectra in NMRPipe[64] and convert the data to a text-file format, then generate a stacked overlay using MATLAB software.

26. **Analysis of the $^{1}$H STE diffusion spectra to evaluate the translational diffusion** Process each $^{1}$H STE diffusion spectrum. Integrate the resonances arising from the ribosomal background (methyl region) for each of the gradient strengths, and plot the integrated signal against the time of acquisition. Determine the noise level of the signal integral. This is the standard deviation calculated from integrated signals that have been randomly selected from 30-35 regions of identical bandwidth within the baseline of the spectra.

27. Determine translational diffusion coefficients of the observed ribosomal resonances using the Stejskal-Tanner equation[70] (Equation 1) which relates the attenuation in signal at a given strength of the pulsed-field gradient to the diffusion coefficient, *D*.

$$\frac{I}{I_o} = \exp\left[-D\gamma^2\sigma^2\delta^2G^2\left(\Delta - \frac{\delta}{3} - \frac{\tau}{2}\right)\right] \quad \text{(Equation 1)}$$

where I and $I_0$ are the intensities at the two gradient strengths, γ is the $^{1}$H gyromagnetic ratio ($2.67522128 \times 10^{8}$ rad $s^{-1}$ $T^{-1}$), σ is the shape factor (0.9 for a square gradient), Δ is the diffusion delay (100 ms), δ is the length of the gradient pair (4 ms), *G* is the gradient strength, τ is the delay between gradient pulses in bipolar gradient pairs, and *D*, the diffusion coefficient. Use either the ratio in intensities of 5% and 95% or 50% and 95% of the total gradient strength, *G* in order to determine a value for the diffusion coefficient *D*.

28. **Determining the period of ribosome stability.** Using the $^{1}$H 1D plots produced in step 25, evaluate over time the methyl resonances arising from the ribosomal background protein, together with the plots of translational diffusion produced in step 27. Determine the timeframe during which these observations remain unchanged and which reports on an intact 70S complex.

29. **Analysis of the $^{13}$C-edited STE or $^{15}$N XSTE (SORDID) spectra to determine the period of nascent chain attachment.** Process each $^{13}$C-edited STE / $^{15}$N XSTE / SORDID diffusion spectrum using NMRPipe software: Repeat analyses as described in step 27, using gradient strengths 5% *G* and 95% *G*. For $^{15}$N XSTE diffusion (or: SORDID diffusion), integrate signals arising from the amide region (7.9-8.4 p.p.m.) in the $^{1}$H dimension. For $^{13}$C-edited STE diffusion, diffusion analysis can be performed on resonances arising from the ribosome (methyl region: 0.8-1 p.p.m. on the $^{1}$H axis) as well as any discrete, well-dispersed resonances arising from the nascent chain that are present in these spectra.

*30.* Determine the noise level of the integrated signal as the standard deviation of the integral of signal in 2-3 regions of identical bandwidth, chosen randomly in baseline parts of the spectrum between 6.5 p.p.m. and 11.5 p.p.m. in the $^{1}$H dimension for $^{15}$N XSTE (or SORDID) diffusion, and between -2 p.p.m. and 1.5 p.p.m. in the $^{1}$H dimension for $^{13}$C-edited

STE diffusion. Average a number of $^{13}$C-edited STE or $^{15}$N XSTE spectra if the uncertainties in diffusion measurements are too large. If this is not possible, refer to step 31.

31. **Analysis of heteronuclear correlation spectra to monitor sample stability.** Process each $^{1}$H-$^{13}$C methyl-TROSY HMQC or $^{1}$H-$^{15}$N/$^{13}$C SOFAST-HMQC spectrum using NMRPipe software, following manufacturer's instructions. Select discrete, unambiguous resonances for subsequent analysis. If the isolated protein has been assigned, identify the RNC resonances by spectral overlay and transfer assignments. Determine peak heights for the resonances of interest, as well as peak heights for any discrete ribosomal bL12 resonances.

32. Determine peak heights of (typically 100) randomly chosen positions in the same chemical shift range as the RNC resonances within a spectrum. The uncertainty of each intensity measurement in step 31 is given by the standard deviation of the noise intensity measurements.

33. Plot averaged peak heights of the resonances arising from the nascent chain and ribosomal protein bL12 over time. Intensity changes are typically indicative of sample breakdown.

**Characterisation of the structural and dynamical properties of the RNC.TIMING 0.5 d**

34. Once the timeframe during which the RNC remains intact has been established using the approaches in steps 24-33, sum the corresponding heteronuclear correlation spectra. A residue-by-residue analysis of the heteronuclear spectra can be undertaken, using 2D correlation spectra by comparing spectra of the isolated protein in the presence of 70S ribosomes, as described in *Experimental design*.

## TROUBLESHOOTING

Troubleshooting advice is provided in Table 1.

Table 1. Troubleshooting

| STEP | PROBLEM | POSSIBLE REASON | POSSIBLE SOLUTION |
|---|---|---|---|
| step 14 | Poor separation of 70S from contaminants during sucrose gradient centrifugation. | -Gradients were overloaded with sample.<br><br>-Gradients not uniform or pre-chilled. | - Load less material and/or increase the number of gradients.<br><br>- Prepare gradients using a gradient former and chill all tubes until required. |
| step 24 | Few or no RNC resonances can be observed. | -The sample concentration is too low, has been compromised<br><br>-Sample not efficiently | -Ensure that the sample is intact (Box 2) and at a concentration in the μM range. Check whether there is signal for bL12 in the methyl region of the spectrum if applicable.<br>- Evaluate the timing of isotope addition to the media |

| | | | |
|---|---|---|---|
| | | isotopically-labelled<br><br>-NMR acquisition parameters do not allow observation of the nascent chain<br><br>- Structural and/or dynamic characteristics of the RNC (e.g. conformational exchange, interaction with the ribosome | -Evaluate and optimise NMR acquisition parameters as required (e.g. acquisition time, sweep widths, temperature).<br><br>-Evaluate the NMR characteristics of the isolated polypeptide and the extent of interaction with 70S ribosomes.<br>-Re-design RNC system as needed |
| step 24 | Large extent of 70S background labelling. | Expression step may have allowed time for the production of labelled 70S particles during exposure to labelled isotopes. | -Optimise expression time for RNC production<br>-Evaluate the use of rifampicin during expression. |
| Box 2 | No or little expression. | Expression conditions need optimising for specific nascent chain. | - Evaluate expression conditions on a small scale, by varying parameters such as *E. coli* cell line/vector, expression time and temperature. Detect RNC expression via western blotting. |
| Box 2 | Low yield. | Poor expression (steps 2-3), poor recovery during preparative steps. | - Collect aliquots throughout expression and purification procedures and use western blotting to troubleshoot.<br>- Re-design RNC to include alternative purification tags (e.g. solubility tags) |
| Box 2 | Multiple bands detected on western blot / Bands on silver stained SDS PAGE do not look like 70S ribosome. | -Poor expression of the RNC (Steps 2-3).<br><br>-Integrity of the RNC sample has been compromised by dissociation/degradation or proteolysis. | - Evaluate RNC expression.<br>- Ensure all buffer compositions are correct.<br><br>- Use online web tools to evaluate possible protease cleavage sites in the nascent chain sequence (using e.g. *PeptideCutter web.**expasy**.org/peptide_cutter/*). Supplement buffers with specific protease inhibitors as necessary. |

**TIMING**

Steps 1- 3: Generation of isotopically-labelled RNCs 2 weeks – 1 month

Steps 4-15: Purification of labelled RNCs by metal affinity chromatography and sucrose density gradient centrifugation 3 d

Steps 16-19: Biochemical analysis of the purified RNC samples 2 d

Steps 20-24: NMR data acquisition and parallel biochemical experiments 1-2 d

Steps 25-33: Analysis of RNC sample integrity over time 2 d

Step 34: Characterisation of the structural and dynamical properties of the RNC 0.5 d

**ANTICIPATED RESULTS**

Following expression (steps 2-3), the cells are lysed (steps 4-5) and the soluble cell lysate is subjected to a 35% (w/v) sucrose cushion from which ~50-100 nmol of ribosomes can be recovered per litre of *E. coli* culture (steps 6-8). The ribosomal suspension (a mixture of RNCs, empty 70S ribosomes, ribosomal subunits and released nascent chains) is applied to a metal affinity column, which recovers the fraction containing RNCs, resulting in 6000-9000 pmol of material (steps 9-12). Further purification using a 10-35% (w/v) high-salt sucrose gradient permits the separation of other contaminating species, including ribosome-associated proteins (steps 13-14 and Fig. 2a, b). Following purification, 3-6 nmol (7-15 mg) of RNCs can typically be purified to homogeneity per litre of culture, representing 6-18% of the total ribosomal population recovered from the cell lysate (step 15). This value is representative of the overall purification yield rather than the extent of SecM translational arrest occurring *in vivo,* which may be significantly greater. Following these preparative steps, the degree of translational arrest in the purified sample, estimated using isolated protein standards of known concentrations, is typically observed to be >90% (steps 16-19 and Fig. 2c, d). Within the RNC sample, the extent of 70S background isotopic labelling is subsequently evaluated using a combination of $^{15}$N (or $^{13}$C) filtered 1D proton and edited 1D proton spectra, in which for the case of uniformly $^{15}$N-labelled samples, the intensity of the envelope of $^{14}$N-bound protons arising from the ribosomal bL12 resonances (unlabelled amides) are compared against that of $^{15}$N-bound protons (labelled amides); an analogous approach is used for uniformly $^{13}$C-labelled samples (step 23). We observe that typically 5-15% of the bL12 protein is isotopically-labelled, and therefore overall, ribosome background labelling of this magnitude contributes only minimally to heteronuclear experiments (Supplementary Fig. 2). Variability in overall RNC yields relates to the nascent chain system, and is thus considered on a case-by-case basis (see Troubleshooting for details).

To illustrate how we can use NMR to observe successive stages of the folding of an emerging nascent chain, here we show two RNC examples from our studies[1] of the biosynthesis of an immunoglobulin domain derived from the multi-domain protein, FLN. These RNCs mimic the progressive emergence and co-translational folding of FLN5, and consist of FLN5 tethered to increasing numbers of residues of the subsequent domain, FLN6[10], and a SecM stalling sequence. In the FLN5+21 RNC construct, the FLN5 domain resides 21 residues from the PTC, which is in the vicinity of the ribosomal exit tunnel. In FLN5+110 RNC, the nascent chain is separated by a significant distance (110 residues) from the PTC[1, 10] (Fig. 4a, b). Resonances in $^{1}$H-$^{15}$N correlation spectra of FLN5+21 RNC give rise to a narrow resonance dispersion in the $^{1}$H dimension consistent with a disordered conformation, while $^{1}$H-$^{13}$C HMQC spectra of [U-$^{2}$H]; Ileδ1-[$^{13}CH_3$]-labelled FLN5+110 RNC show dispersed resonances characteristic of a well-folded protein, as well as intense overlapped resonances characteristic of disordered conformations.

To ensure that these resonances arise from a ribosome-attached nascent chain, examination of both western blot and diffusion analyses is recommended (steps 29-30 and Box

2). In the case of the disordered FLN5+21 RNC sample, western blot analyses reveal a significant change in the intensity of the tRNA-bound nascent chain band after t=2.1 h (Fig. 4c) as observed in the anti-His blot (top), and after t=5.9 h in an anti-SecM blot (bottom). Similarly, $^{15}$N XSTE diffusion data reveal changes in *D* beyond t=2.1 h, suggesting that within this 2 h timeframe, the RNC is intact (Fig. 4e). For the FLN5+110 RNC, both the anti-His and anti-SecM western blots (Fig. 4d) indicate that the tRNA-bound nascent chain remains stable throughout an NMR acquisition period of 17 h, beyond which, NMR data are not included in the analysis. Indeed, lower molecular weight bands observable in the anti-SecM blot at t=32 h are consistent with truncation of the nascent chain. In addition, the diffusion coefficient, *D*, can also be determined from $^{13}$C-edited STE experiments on discrete resonances arising exclusively from the nascent chain, and reports an intact RNC ($D$=1.5 ± 0.3 x$10^{-11}$ $m^2s^{-1}$) until t=17 h (Fig. 4f). Generally, changes in the intensity of the tRNA-bound nascent chain band in excess of 10% of the original intensity are regarded as significant, as these could give rise to interfering NMR signals. These intensity changes are also often concomitant with the appearance of lower molecular weight bands that we attribute to nascent chain release (e.g. overcoming translational arrest or proteolysis), and an increase in the diffusion coefficient associated with the nascent chain resonances. The timeframe during which the nascent chain is stable within a given RNC varies between sample preparations and the integrity of each sample during the course of its NMR acquisition is therefore considered on an individual basis.

Structural NMR spectra (such as heteronuclear correlation spectra, RDC or dynamics data) reflecting intact RNCs are typically summed and analysis of the structural and dynamical properties of the RNC undertaken. In this example the shortest nascent chain length, FLN5+21 RNC, shows disordered resonances in $^{1}$H-$^{15}$N correlation spectra which overlay closely with those of a corresponding disordered isolated variant, (termed FLN5Δ12, Fig. 4a). This suggests similar conformations of the two samples and a disordered FLN5 nascent chain when the domain is close to the ribosomal exit. In contrast, once the linker length has increased to 110 residues, the resonances observed for [U-$^{2}$H]; Ileδ1-[$^{13}CH_3$]-labelled FLN5+110 RNC were found to overlay closely with those of isolated natively-folded FLN5. Four dispersed methyl resonances (corresponding to I738, I743, I674, and I695, within 0.01 p.p.m. in the $^{1}$H dimension) can be identified, and where I748 is discernible but overlaps in most spectra with resonances arising from the ribosomal stalk, resulting from background labelling (Fig. 4b). These data demonstrate that FLN5+110 RNC adopts a native FLN5 fold.

These experiments have provided the foundation for examining “structural snapshots” of a nascent chain during synthesis and folding on the ribosome. This will allow the determinants of co-translational protein folding and the influence of scenarios unique to the emerging nascent chain including the vectorial emergence of the amino acid sequence, the presence of the

ribosome, and the role of molecular chaperones to be explored at a residue-specific level and at high resolution.

**Author contributions** A.M.E.C., H.M.M.L., C.A.W., J.C. and L.D.C. designed the study. A.M.E.C., H.M.M.L., M.E.K., X.W., C.A.W., A.D., A.L.R. and L.D.C. performed the research. A.M.E.C., C.A.W., J.C. and L.D.C. wrote the paper. All authors discussed the results and contributed to the final version of the paper.

**Acknowledgements** We thank Bernd Bukau (Ruprecht-Karls-Universität Heidelberg) for anti-SecM antibody. We thank the staff and acknowledge use of the MRC NMR Centre at the Crick Institute for their Biomolecular NMR facilities. This work was supported by a New Investigators Award BBSRC BBG0156511 and a Wellcome Trust Investigator Award, 097806/Z/11/Z (J.C.); an AlphaOne Foundation grant (L.D.C); A.L.R is a NH&MRC C.J Martin Fellow.

**Competing financial interests** The authors declare that they have no competing financial interests.

## References

1. Cabrita, L.D. et al. A structural ensemble of a ribosome-nascent chain complex during cotranslational protein folding. *Nat Struct Mol Biol* **23**, 278-285 (2016).
2. Cabrita, L.D., Dobson, C.M. & Christodoulou, J. Protein folding on the ribosome. *Current Opinion in Structural Biology* **20**, 33-45 (2010).
3. Nicola, A.V., Chen, W. & Helenius, A. Co-translational folding of an alphavirus capsid protein in the cytosol of living cells. *Nature Cell Biology* **1**, 341-345 (1999).
4. Hoffmann, A. et al. Concerted action of the ribosome and the associated chaperone trigger factor confines nascent polypeptide folding. *Molecular Cell* **48**, 63-74 (2012).
5. Ito, K. & Chiba, S. Arrest peptides: cis-acting modulators of translation. *Annu. Rev. Biochem.* **82**, 171-202 (2013).
6. Kelkar, D.A., Khushoo, A., Yang, Z. & Skach, W.R. Kinetic analysis of ribosome-bound fluorescent proteins reveals an early, stable, cotranslational folding intermediate. *The Journal of biological chemistry* **287**, 2568-2578 (2012).
7. Kim, S.J. et al. Protein folding. Translational tuning optimizes nascent protein folding in cells. *Science* **348**, 444-448 (2015).
8. Seidelt, B. et al. Structural Insight into Nascent Polypeptide Chain-Mediated Translational Stalling. *Science* **326**, 1412-1415 (2009).
9. Bhushan, S. et al. SecM-Stalled Ribosomes Adopt an Altered Geometry at the Peptidyl Transferase Center. *PLoS Biology* **9**, e1000581 (2011).
10. Cabrita, L.D., Hsu, S.-T.D., Launay, H., Dobson, C.M. & Christodoulou, J. Probing ribosome-nascent chain complexes produced in vivo by NMR spectroscopy. *Proceedings of the National Academy of Sciences of the United States of America* **106**, 22239-22244 (2009).
11. Evans, M.S., Ugrinov, K.G., Frese, M.-A. & Clark, P.L. Homogeneous stalled ribosome nascent chain complexes produced in vivo or in vitro. *Nature Methods* **2**, 757-762 (2005).
12. Nakatogawa, H. & Ito, K. The ribosomal exit tunnel functions as a discriminating gate. *Cell* **108**, 629-636 (2002).
13. Ugrinov, K.G. & Clark, P.L. Cotranslational Folding Increases GFP Folding Yield. *Biophysical Journal* **98**, 1312-1320 (2010).
14. Kudlicki, W., Chirgwin, J., Kramer, G. & Hardesty, B. Folding of an enzyme into an active conformation while bound as peptidyl-tRNA to the ribosome. *Biochemistry* **34**, 14284-14287 (1995).
15. Evans, M.S., Sander, I.M. & Clark, P.L. Cotranslational Folding Promotes beta-Helix Formation and Avoids Aggregation In Vivo. *Journal of Molecular Biology* **383**, 683-692 (2008).

16. Tsalkova, T., Odom, O.W., Kramer, G. & Hardesty, B. Different conformations of nascent peptides on ribosomes. *J Mol Biol* **278**, 713-23 (1998).
17. Kleizen, B., van Vlijmen, T., de Jonge, H.R. & Braakman, I. Folding of CFTR is predominantly cotranslational. *Molecular Cell* **20**, 277-287 (2005).
18. Frydman, J., Erdjument-Bromage, H., Tempst, P. & Hartl, F.U. Co-translational domain folding as the structural basis for the rapid de novo folding of firefly luciferase. *Nat. Struct. Biol.* **6**, 697-705 (1999).
19. Friguet, B., Djavadi-Ohaniance, L., King, J. & Goldberg, M.E. In vitro and ribosome-bound folding intermediates of P22 tailspike protein detected with monoclonal antibodies. *J. Biol. Chem.* **269**, 15945-15949 (1994).
20. Speed, M.A., Morshead, T., Wang, D.I. & King, J. Conformation of P22 tailspike folding and aggregation intermediates probed by monoclonal antibodies. *Protein Sci.* **6**, 99-108 (1997).
21. Zhang, G., Hubalewska, M. & Ignatova, Z. Transient ribosomal attenuation coordinates protein synthesis and co-translational folding. *Nat Struct Mol Biol* **16**, 274-80 (2009).
22. Holtkamp, W. et al. Cotranslational protein folding on the ribosome monitored in real time. *Science* **350**, 1104-1107 (2015).
23. Woolhead, C.A., McCormick, P.J. & Johnson, A.E. Nascent membrane and secretory proteins differ in FRET-detected folding far inside the ribosome and in their exposure to ribosomal proteins. *Cell* **116**, 725-736 (2004).
24. Lu, J. & Deutsch, C. Secondary Structure Formation of a Transmembrane Segment in Kv Channels †. *Biochemistry* **44**, 8230-8243 (2005).
25. Kaiser, C.M., Goldman, D.H., Chodera, J.D., Tinoco, I. & Bustamante, C. The Ribosome Modulates Nascent Protein Folding. *Science* **334**, 1723-1727 (2011).
26. Knight, A.M. et al. Electrostatic effect of the ribosomal surface on nascent polypeptide dynamics. *ACS Chemical Biology* **8**, 1195-1204 (2013).
27. Sander, I.M., Chaney, J.L. & Clark, P.L. Expanding Anfinsen's principle: contributions of synonymous codon selection to rational protein design. *J Am Chem Soc* **136**, 858-61 (2014).
28. Fedyunin, I. et al. tRNA concentration fine tunes protein solubility. *FEBS Letters* **586**, 3336-3340 (2012).
29. Corazza, A. et al. Native-unlike long-lived intermediates along the folding pathway of the amyloidogenic protein beta2-microglobulin revealed by real-time two-dimensional NMR. *Journal of Biological Chemistry* **285**, 5827-5835 (2010).
30. Kaiser, C.M. et al. Real-time observation of trigger factor function on translating ribosomes. *Nature* **444**, 455-60 (2006).
31. Nilsson, O.B., Müller-Lucks, A., Kramer, G., Bukau, B. & von Heijne, G. Trigger Factor Reduces the Force Exerted on the Nascent Chain by a Cotranslationally Folding Protein. *J. Mol. Biol.* (2016).
32. Gabashvili, I.S. et al. Solution structure of the E. coli 70S ribosome at 11.5 A resolution. *Cell* **100**, 537-549 (2000).
33. Stark, H. et al. Visualization of elongation factor Tu on the Escherichia coli ribosome. *Nature* **389**, 403-406 (1997).
34. Nissen, P., Hansen, J., Ban, N., Moore, P.B. & Steitz, T.A. The structural basis of ribosome activity in peptide bond synthesis. *Science* **289**, 920-930 (2000).
35. Ban, N., Nissen, P., Hansen, J., Moore, P.B. & Steitz, T.A. The complete atomic structure of the large ribosomal subunit at 2.4 A resolution. *Science* **289**, 905-920 (2000).
36. Gao, Y.-G. et al. The structure of the ribosome with elongation factor G trapped in the posttranslocational state. *Science* **326**, 694-699 (2009).
37. Selmer, M. et al. Structure of the 70S ribosome complexed with mRNA and tRNA. *Science* **313**, 1935-1942 (2006).
38. Bhushan, S. et al. alpha-Helical nascent polypeptide chains visualized within distinct regions of the ribosomal exit tunnel. *Nature Structural Molecular Biology* **17**, 313-317 (2010).

39. Hsu, S.-T.D. et al. Structure and dynamics of a ribosome-bound nascent chain by NMR spectroscopy. *Proceedings of the National Academy of Sciences of the United States of America* **104**, 16516-16521 (2007).
40. Hsu, S.T., Cabrita, L.D., Fucini, P., Christodoulou, J. & Dobson, C.M. Probing side-chain dynamics of a ribosome-bound nascent chain using methyl NMR spectroscopy. *J Am Chem Soc* **131**, 8366-7 (2009).
41. Eichmann, C., Preissler, S., Riek, R. & Deuerling, E. Cotranslational structure acquisition of nascent polypeptides monitored by NMR spectroscopy. *Proceedings of the National Academy of Sciences of the United States of America* **107**, 9111-9116 (2010).
42. Nilsson, O.B. et al. Cotranslational Protein Folding inside the Ribosome Exit Tunnel. *Cell Rep* **12**, 1533-1540 (2015).
43. Christodoulou, J. et al. Heteronuclear NMR investigations of dynamic regions of intact Escherichia coli ribosomes. *Proceedings of the National Academy of Sciences of the United States of America* **101**, 10949-10954 (2004).
44. Mulder, F.A.A. et al. in Biochemistry 5930-5936 (2004).
45. Rutkowska, A. et al. Large-scale purification of ribosome-nascent chain complexes for biochemical and structural studies. *FEBS Lett* **583**, 2407-13 (2009).
46. Hsu, S.T., Cabrita, L.D., Fucini, P., Dobson, C.M. & Christodoulou, J. Structure, dynamics and folding of an immunoglobulin domain of the gelation factor (ABP-120) from Dictyostelium discoideum. *J Mol Biol* **388**, 865-79 (2009).
47. Deckert, A.W., Christopher A.; Wlodarski, Tomasz; Wentink, Anne S.; Wang, Xiaolin; Kirkpatrick, John P.; Paton, Jack F. S.; Camilloni, Carlo; Kukic, Predrag; Dobson, Christopher M.; Vendruscolo, Michele; Cabrita, Lisa D.; Christodoulou John. Structural characterization of the interaction of α-synuclein nascent chains with the ribosomal surface and trigger factor. *Proceedings of the National Academy of Sciences* **113**, 5012-5017 (2016).
48. Studier, F.W. Protein production by auto-induction in high density shaking cultures. *Protein Expr Purif* **41**, 207-34 (2005).
49. Spedding, G. Isolation and analysis of ribosomes from prokaryotes, eukaryotes, and organelles. *Ribosomes and Protein Synthesis*, 1-29 (1990).
50. Bergemann, K. & Nierhaus, K.H. Spontaneous, elongation factor G independent translocation of Escherichia coli ribosomes. *J. Biol. Chem.* **258**, 15105-15113 (1983).
51. Fredrick, K. & Noller, H.F. Catalysis of ribosomal translocation by sparsomycin. *Science* **300**, 1159-1162 (2003).
52. Hsu, S.-T.D. et al. in Proceedings of the National Academy of Sciences of the United States of America 16516-16521 (2007).
53. Bai, Y., Milne, J.S., Mayne, L. & Englander, S.W. Primary structure effects on peptide group hydrogen exchange. *Proteins* **17**, 75-86 (1993).
54. Deusser, E. & Wittmann, H.G. Ribosomal proteins: variation of the protein composition in Escherichia coli ribosomes as function of growth rate. *Nature* **238**, 269-270 (1972).
55. Rostom, A.A. et al. Detection and selective dissociation of intact ribosomes in a mass spectrometer. *Proc Natl Acad Sci U S A* **97**, 5185-5190 (2000).
56. Ramagopal, S. & Subramanian, A.R. Alteration in the acetylation level of ribosomal protein L12 during growth cycle of Escherichia coli. *PNAS* **71**, 2136-2140 (1974).
57. Lu, J. & Deutsch, C. Folding zones inside the ribosomal exit tunnel. *Nat Struct Mol Biol* **12**, 1123-1129 (2005).
58. Zhang, G., Hubalewska, M. & Ignatova, Z. Transient ribosomal attenuation coordinates protein synthesis and co-translational folding. *Nat Struct Mol Biol* **16**, 274-280 (2009).
59. Kaiser, C.M. et al. Real-time observation of trigger factor function on translating ribosomes. *Nature* **444**, 455-460 (2006).
60. Chan, S.H.S., Waudby, C.A., Cassaignau, A.M.E., Cabrita, L.D. & Christodoulou, J. Increasing the sensitivity of NMR diffusion measurements by paramagnetic longitudinal relaxation enhancement, with application to ribosome-nascent chain complexes. *J Biomol NMR* **63**, 1-13 (2015).

61. Kay, L.E. Solution NMR spectroscopy of supra-molecular systems, why bother? A methyl-TROSY view. *Journal of Magnetic Resonance* **210**, 159-170 (2011).
62. Wiesner, S. & Sprangers, R. Methyl groups as NMR probes for biomolecular interactions. *Current Opinion in Structural Biology* **35**, 60-67 (2015).
63. Tugarinov, V., Kanelis, V. & Kay, L.E. Isotope labeling strategies for the study of high-molecular-weight proteins by solution NMR spectroscopy. *Nature protocols* **1**, 749-754 (2006).
64. Delaglio, F. et al. NMRPipe: a multidimensional spectral processing system based on UNIX pipes. *J Biomol NMR* **6**, 277-293 (1995).
65. Vranken, W.F. et al. The CCPN data model for NMR spectroscopy: development of a software pipeline. *Proteins* **59**, 687-696 (2005).
66. Sivashanmugam, A. et al. Practical protocols for production of very high yields of recombinant proteins using Escherichia coli. *Protein Sci* **18**, 936-48 (2009).
67. Hill, W.E., Rossetti, G.P. & Van Holde, K.E. Physical studies of ribosomes from Escherichia coli. *J Mol Biol* **44**, 263-77 (1969).
68. Mahmood, T. & Yang, P.-C. Western blot: technique, theory, and trouble shooting. *N Am J Med Sci* **4**, 429-434 (2012).
69. Augustyniak, R., Ferrage, F., Damblon, C., Bodenhausen, G. & Pelupessy, P. Efficient determination of diffusion coefficients by monitoring transport during recovery delays in NMR. *Chem. Commun.* **48**, 5307-5309 (2012).
70. Stejskal, E.O. & Tanner, J.E. Spin diffusion measurements: Spin echoes in the presence of a time-dependent field gradient. *J. Chem. Phys.* **42**, 288 (1965).
71. Waudby, C.A., Launay, H., Cabrita, L.D. & Christodoulou, J. Protein folding on the ribosome studied using NMR spectroscopy. *Progress in nuclear magnetic resonance spectroscopy* **74**, 57-75 (2013).
72. Waudby, C.A. & Christodoulou, J. An analysis of NMR sensitivity enhancements obtained using non-uniform weighted sampling, and the application to protein NMR. *Journal of Magnetic Resonance* **219**, 46-52 (2012).

**Box 1 Sensitivity versus resolution**

The upper limit of 70S ribosome particle working concentration is ~10 μM which corresponds to a very high 24 mg/mL of 70S in solution. This concentration represents a major sensitivity challenge for modern biological NMR investigation in particular when combined with the limited stability of RNCs in solution. In RNC NMR studies it is crucial to optimise proposed NMR experiments in order to maximise signal[71]. The sensitivity of 2D NMR experiments for a fixed total acquisition time and spectral resolution is determined by several factors (see inset figure): [NC] is the nascent chain concentration, T is the total acquisition time, $B_0$ is the magnetic field strength, $T_2$ is the transverse relaxation rate in the indirect dimension, and $t_{1,max}$ is the maximum evolution time in the indirect dimension, which is proportional to the frequency resolution. The nascent chain concentration [NC], is the limiting factor in determining the overall sensitivity. By contrast, there are diminishing returns for increases in the total acquisition time $T$, as a result of the $T^{1/2}$ dependence. The frequency resolution in the indirect dimension (as determined by the maximum evolution time $t_{1,max}$) is another key choice, as there is an inevitable compromise between sensitivity and resolution. We optimise $t_{1,max}$ using the analogous isolated protein of the RNC system and, in the first instance, acquire 2D heteronuclear spectra for an uncharacterised RNC using the lowest acceptable resolution (e.g. $t_{1,max}$ = 14.1 ms) to maximise the overall NMR signal. Acquisition at higher field strengths is also likely to be beneficial as, in addition to the direct sensitivity gains due to the increased field strength, spectra can be acquired with identical chemical shift resolution (in p.p.m.) but with shorter evolution times, ($t_{1,max}$ and $t_{2,max}$), thereby reducing relaxation losses. However, for some systems, it is possible that chemical exchange-induced line broadening may reduce sensitivity of some resonances at higher fields. This should be assessed on a case-by-case basis, ideally using an isolated RNC analogue, in order to determine the combination of field strength and evolution times that optimise sensitivity or resolution as required. In our own hands, we have only observed positive effects on increasing the field strength from 700 to 950 MHz, and as 1.2 GHz fields are likely to become available in the next few years, the prospect of further improvements in sensitivity is encouraging. In addition, by implementing *in advance* an appropriate apodization function, the use of non-uniform weighted sampling methods can provide additional sensitivity improvements of 10–20%, without distortion of the resulting spectra[72]. Further recent developments include the use of soluble paramagnetic compounds that can be introduced into NMR samples, strongly accelerating longitudinal relaxation and hence increasing sensitivity at a cost of only little relative effect on transverse relaxation. This paramagnetic longitudinal relaxation enhancement (PLRE) effect has been shown to yield sensitivity gains of up to 85% on RNC samples when using the Ni(II) chelate NiDO2A[60].

**Box 1 inset figure.**

END OF BOX 1

**Box 2 Analysis of RNC sample integrity during NMR acquisition TIMING 1.5 d**

1. Run the samples collected during NMR acquisition on a 12-15% polyacrylamide SDS PAGE gel. Include the following control samples: purified 70S ribosome to check for nonspecific antibody binding, and a sample of RNase A-treated RNC as a control for released nascent chain.
2. Perform a western blot using an anti-His, anti-SecM and/or other nascent chain-specific antibody.

3. Monitor for the presence of a band corresponding to the molecular weight of the tRNA-bound nascent chain, as well as for the appearance of released nascent chains.
4. Use densitometry software to measure the tRNA-bound nascent chain for each sample, and plot the raw value relative to time

**END OF BOX 2**

**Figures**

**Figure 1. General scheme for structural studies of RNCs by NMR spectroscopy**. An outline of RNC design, preparation, and subsequent analysis by NMR spectroscopy and biochemistry, as described in the *Overview of the Procedure* section.

**Figure 2. Biochemical assessment of purified RNCs**

**a** Following $Ni^{2+}$ metal affinity purification, the RNCs are subjected to a 10-35% (w/v) sucrose gradient. The fractionation profile is monitored by $OD_{254nm}$. **b** The resulting fractions are examined by SDS PAGE for the pattern corresponding to intact 70S ribosomal proteins and boxed in red are the pooled fractions. The typical banding pattern consistent with 70S ribosomal proteins includes S1 (60 kDa), and a collection of ribosomal proteins <30 kDa.

**c** An anti-His western blot of a FLN5 RNC (FLN5+67 RNC) following purification, showing tRNA-bound and released nascent chain, which differ in molecular weight by ~17-20 kDa. **d** For nascent chain occupancy estimation, 1-2 pmol of RNC (ribosomal concentration) and varying concentrations of isolated FLN5 (0.25-2.5 pmol) are blotted on the same membrane. A standard curve (inset) uses the band intensities derived from densitometry analyses of isolated FLN5 concentration standards.

**Figure 3. NMR analysis of RNC integrity**

**a** $^{15}N$ diffusion measurements: *top* The RNC amide envelope is shown at two gradient strengths (5 and 95% *G*), at three different timepoints during NMR acquisition. *middle* The integrated amide envelope signal is shown throughout NMR acquisition, highlighting the timepoints for which the spectra are shown on top. *bottom* The calculated diffusion coefficient *D* is shown throughout NMR acquisition, again highlighting the timepoints for which the spectra are shown on top. **b** The methyl region (0.7-1 p.p.m.) in $^{1}H$ 1Ds contains predominantly resonances arising from the ribosomal protein bL12, which can be monitored as a probe for the integrity of the ribosome. The methyl region of the $^{1}H$ 1D spectrum is assessed over the time course of NMR acquisition. **c** Integrated signal between 0.79 and 0.97 p.p.m. of $^{1}H$-STE diffusion spectra of FLN5 RNC recorded at three gradient strengths. 0% *G* represents the signal observed in $^{1}H$ 1Ds. The diffusion coefficient of the RNC can be determined from the ratio of the integrated signals between 50% *G* and 95% *G*, plotted over time. The diffusion coefficient expected for an intact

ribosomal particle is indicated by the shaded area ($D$ = 1.7-2.2 $10^{-11}$ $m^2s^{-1}$). **d** Plot of the mean intensities observed in $^{1}H$-$^{15}N$ HMQCs of Dom5+47 RNC over time, corresponding to natively folded FLN5. **e** Comparison of the $^{1}H$-$^{15}N$ SOFAST HMQC at the start of acquisition (t = 0-8 h) and at the end of acquisition (t = 87-95 h), highlighting the appearance of folded FLN5 (circled), which we attribute to degradation of the sample through release. Disordered FLN5 can also be detected in the central region of the spectrum at t = 87-95 h, which we attribute to proteolysis.

**Figure 4. Heteronuclear spectra of RNCs and monitoring of RNC integrity**

The orthogonal approaches used to evaluate RNC integrity are shown for **a** U-$^{15}N$-labelled FLN5+21 RNC and **b** [U-$^{2}H$]; Ileδ1-[$^{13}CH_3$]-labelled FLN5+110 RNC. Schematic of the DNA construct design and RNC complexes are shown, as well as heteronuclear correlation spectra of the RNCs: **a** $^{1}H$-$^{15}N$ SOFAST-HMQC spectrum of FLN5+21 RNC (black), a $^{1}H$-$^{15}N$ correlation spectrum of a C-terminally truncated FLN5 sample (FLN5Δ12) (red), and an overlay of both, which enables assignment of the RNC resonances by attribution as indicated. **b** $^{1}H$-$^{13}C$ HMQC spectrum of folded FLN5+110 RNC (black), a $^{1}H$-$^{13}C$ HMQC of isolated FLN5 (red) and an overlay of both, which enables assignment of the RNC resonances by attribution. The cross-peaks that overlay with isoleucine resonances arising from folded FLN5, as well as those arising from the background labelled ribosome, are indicated. **c** and **d** Western blot analyses of the samples of the RNCs over the time course of NMR acquisition: anti-His (top), and anti-SecM (bottom). **e** $^{15}N$ X-STE spectra of FLN5+21 RNC recorded at two gradient strengths (5 and 95% $G$). Changes in diffusion coefficient values over the course of the NMR. **f** $^{13}C$ edited STE diffusion spectra of FLN5+110 RNC recorded at two gradient strengths. The translational diffusion coefficient associated with the dispersed isoleucine resonances is shown over the time course of NMR acquisition. The timeframe during which the nascent chain is shown to be attached to the ribosome is indicated by a grey shaded area. *These data have been adapted from ref. [1]: Figure 3 and Supplementary Figures 2 and 3.*

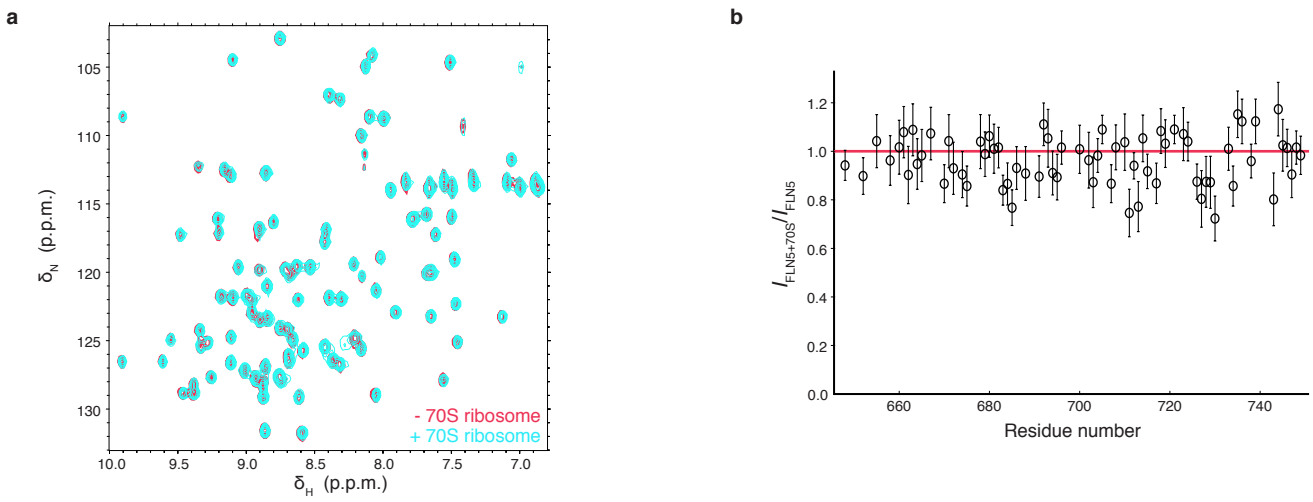


**Supplementary Figure 1**

2D correlation spectra of FLN5 in the presence of 70S ribosomes

**a** A representative region of the SOFAST 2D correlation spectrum overlay of 5 μM $^{15}$N-labelled FLN5 in the absence (red) and presence (cyan) of 5 μM 70S ribosomes. **b** The relative intensities of an equimolar sample of FLN5 and 70S ribosomes (5 μM) vs. FLN5 alone (5 μM), plotted against primary sequence, shows that the intensities of FLN5 resonances remain unchanged in the presence of ribosomes, making it a tractable system for RNC studies. The analogous study can be undertaken with the unfolded polypeptide. Errors are derived from spectral noise from one single measurement. Adapted from ref. 1 with permission from Nature Publishing Group.

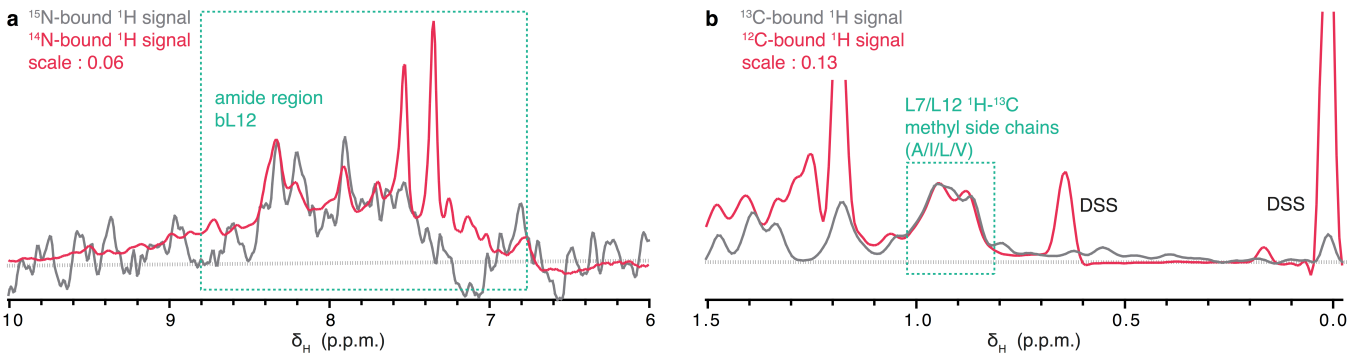


**Supplementary Figure 2**

Assessment of ribosome background labelling

To assess the level of ribosomal background labelling within RNC samples, $^{15}N/^{13}C$ filtered $^{1}H$ 1D (red) and $^{15}N/^{13}C$ edited $^{1}H$ 1D (grey) spectra are collected. The intensity of the $^{1}H$ envelope of bL12 resonances bound to $^{14}N$ ($^{15}N/^{13}C$ filtered $^{1}H$ 1D) is matched by scaling to that of $^{15}N$-bound protons ($^{15}N/^{13}C$ edited $^{1}H$ 1D) in order to quantify the ratio of unlabelled to labelled species. **a** Intensity profiles of amide resonances in $^{15}N$ filtered $^{1}H$ 1D (red) and $^{15}N$ $^{1}H$ edited 1D (grey) spectra from a $^{15}N$-labelled RNC, in which the background labelling amounts to ~6%. **b** Intensity profiles of methyl resonances in $^{13}C$ filtered $^{1}H$ 1D (red) and $^{13}C$ edited $^{1}H$ 1D (grey) spectra from a $^{13}C$-labelled RNC. We determine that ~13% of its bL12 resonances are labelled.